Microfluidic Assembly of Homogeneous and Janus Colloid-Filled Hydrogel Granules

Robert F. Shepherd,[†,‡] Jacinta C. Conrad,[‡,§] Summer K. Rhodes,[†,‡] Darren R. Link,[⊥] Manuel Marquez,[#,||,▽] David A. Weitz,[⊥] and Jennifer A. Lewis*[,†,‡]

Frederick Seitz Materials Research Laboratory, University of Illinois, Urbana, Illinois 61801, Materials Science and Engineering Department, University of Illinois, Urbana, Illinois 61801, INEST Group Postgraduate Program, Philip Morris USA, Richmond, Virginia 23234, Division of Engineering and Applied Science, Harvard University, Cambridge, Massachusetts 02139, NIST Center for Theoretical and Computational Nanosciences, Gaithersburg, Maryland 20899, Harrington Department Bioengineering, Arizona State University, Tempe, Arizona 85287, and Research Center, Philip Morris USA, 4201 Commerce Road, Richmond, Virginia 23234

Received March 21, 2006. In Final Form: August 15, 2006

The microfluidic assembly of colloid-filled hydrogel granules of varying shape and composition is described. First, drops are formed by shearing a concentrated colloidal microsphere−acrylamide suspension in a continuous oil phase using a sheath-flow device. Both homogeneous and Janus (hemispherically distinct) spheres and disks are produced by confining the assembled drops in microchannels of varying geometry. Next, photopolymerization is carried out shortly after drop breakup to preserve their morphology. Representative wet and dried granules are characterized using fluorescence and scanning electron microscopy, respectively. Our approach offers a facile route for assembling colloid-filled hydrogel granules with controlled shape and composition.

Introduction

Colloidal granules are widely utilized as feedstock in the ceramic,[1,2] food,[3] cosmetic,[4] and pharmaceutical[5] industries. In such applications, primary particles in the colloidal size range ($\leq 1\ \mu$m) are intentionally granulated to overcome transport and processing problems such as wall-stick, health hazards from inhalation, and inefficient compaction into pills, tablets, or other forms.[6] Many methods exist for producing wet and dry colloidal granules, including fluid bed granulation,[7] high shear mixer granulation,[8] and spray drying[2]. However, none provide adequate control over granule size, size distribution, shape, or composition, as required for emerging applications such as designer pharmaceuticals[9,10] and optical display technologies.[11]

A new route to granulation is suggested by the emergence of microfluidic techniques that allow the formation of monodisperse emulsion drops by coflowing immiscible fluids at low Reynolds numbers.[12−16] Using this approach, both pure hydrogel[17,18] and polymeric particles[19−22] ($\sim$10−200 μm in diameter) have been produced via in situ photopolymerization of monomeric drops in the form of either homogeneous[17−22] or Janus particles[23−26] and discoids.[19−22] In addition, microfluidic devices have been used to synthesize colloids[27] and to aggregate colloidal particles into photonic balls using extremely dilute suspensions ($\phi \leq 0.01$).[28] However, the guided assembly of dense colloidal suspensions within microfluidic devices has not been explored.

In this letter, we report a scalable microfluidic assembly route for creating monodisperse colloid-filled hydrogel granules of tunable size, geometry, and composition. We exploit the physics of laminar flow in microchannels to first generate drops composed

* Corresponding author. E-mail: jalewis@uiuc.edu.
† Frederick Seitz Materials Research Laboratory, University of Illinois.
‡ Materials Science and Engineering Department, University of Illinois.
§ INEST Group Postgraduate Program, Philip Morris USA (INEST = Interdisciplinary Network of Emerging Science and Technologies).
⊥ Harvard University.
NIST Center for Theoretical and Computational Nanosciences.
|| Arizona State University.
▽ Research Center, Philip Morris USA.

(1) Lewis, J. A. *J. Am. Ceram. Soc.* **2000**, *83* (10), 2341−2359.
(2) Lukasiewicz, S. J. *J. Am. Ceram. Soc.* **1989**, *72* (4), 617−624.
(3) Hogekamp, S.; Stang, M.; Schubert, H. *Chem. Eng. Process.* 1994, *33*, 313−318.
(4) Oulahna, D.; Cordier, F.; Galet, L.; Dodds, J. A. *Powder Technol.* **2003**, *130*, 238−246.
(5) Simons, S. J. R.; Rosetti, D.; Pagliai, P.; Ward, R.; Fitzpatrick, S. *Powder Technol.* **2004**, *140*, 280−289.
(6) Saleh, K.; Vialatte, L.; Guigon, P. *Chem. Eng. Sci.* **2005**, *60*, 3763−3775.
(7) Cryer, S. A. *AIChE J.* **1999**, *45* (10), 2069−2078.
(8) Darelius, A.; Rasmuson, A.; Bjorn, I. N.; Folestad, S. *Powder Technol.* **2005**, *160* (3), 209−218.
(9) York, P. *Drug Dev. Ind. Pharm.* **1992**, *18* (6−7), 677−721.
(10) Collins, F. S.; McKusick, V. A. *J. Am. Med. Assoc.* **2001**, *285* (5), 540−544.
(11) Chen, Y.; Au, J.; Kazlas, P.; Ritenour, A.; Gates, H.; McCreary, M. *Nature* **2003**, *423* (6936), 136.
(12) Umbanhowar, P. B.; Prasad, V.; Weitz, D. A. *Langmuir* **2000**, *16*, 347−351.
(13) Thorsen, T.; Roberts, R. W.; Arnold, F. H.; Quake, S. R. *Phys. Rev. Lett.* **2001**, *86* (18), 4163−4166.
(14) Anna, S. L.; Bontoux, N.; Stone, H. A. *Appl. Phys. Lett.* **2003**, *82* (3), 364−366.
(15) Link, D. R.; Anna, S. L.; Weitz, D. A.; Stone, H. A. *Phys. Rev. Lett.* **2004**, *92* (5), 054503.
(16) Song, H.; Tice, J. D.; Ismagilov, R. F. *Angew. Chem., Int. Ed.* **2003**, *42* (7), 767−772.
(17) Jeong, W. J.; Kim, J. Y.; Choo, J.; Lee, E. K.; Han, C. S.; Beebe, D. J.; Seong, G. H.; Lee, S. H. *Langmuir* **2005**, *21*, 3738−3741.
(18) De Geest, B.; Urbanski, J. P.; Thorsen, T.; Demeester, J.; De Smedt, S. C. *Langmuir* **2005**, *21* (23), 10275−10279.
(19) Dendukuri, D.; Tsoi, K.; Hatton, T. A.; Doyle, P. S. *Langmuir* **2005**, *21*, 2113−2116.
(20) Xu, S.; Nie, Z.; Seo, M.; Lewis, P.; Kumacheva, E.; Stone, H.; Garstecki, P.; Weibel, D.; Gitlin, I.; Whitesides, G. *Angew. Chem., Int. Ed.* **2005**, *44*, 724−728.
(21) Seo, M.; Nie, Z.; Xu, S.; Mok, M.; Lewis, P. C.; Graham, R.; Kumacheva, E. *Langmuir* **2005**, *21* (25), 11614−11622.
(22) Seo, M.; Nie, Z.; Xu, S.; Lewis, P. C.; Kumacheva, E. *Langmuir* **2005**, *21* (11), 4773−4775.
(23) Roh, K.; Martin, D.; Lahann, J. *Nat. Mater.* **2005**, *4* (10), 759−763.
(24) Dendukuri, D.; Pregibon, D.; Collins, J.; Hatton, T.; Doyle, P. *Nat. Mater.* **2006**, *5* (5), 365−369.
(25) Nie, Z.; Li, W.; Seo, M.; Xu, S.; Kumacheva, E. *J. Am. Chem. Soc.* **2006**, *128* (29), 9408−9412.
(26) Nisisako, T.; Torii, T.; Higuchi, T. *Chem. Eng. J.* **2004**, *101*, 23−29.
(27) Khan, S. A.; Gunther, A.; Schmidt, M. A.; Jensen, K. F. *Langmuir* **2004**, *20* (20), 8604−8611.
(28) Yi, G.-R.; Thorsen, T.; Manoharan, V. N.; Hwang, M. J.; Jeon, S.-J.; Pine, D. J.; Quake, S. R.; Yang, S. M. *Adv. Mater.* **2003**, *15* (15), 1300−1304.

10.1021/la060759+ CCC: $33.50
Published on Web 09/15/2006

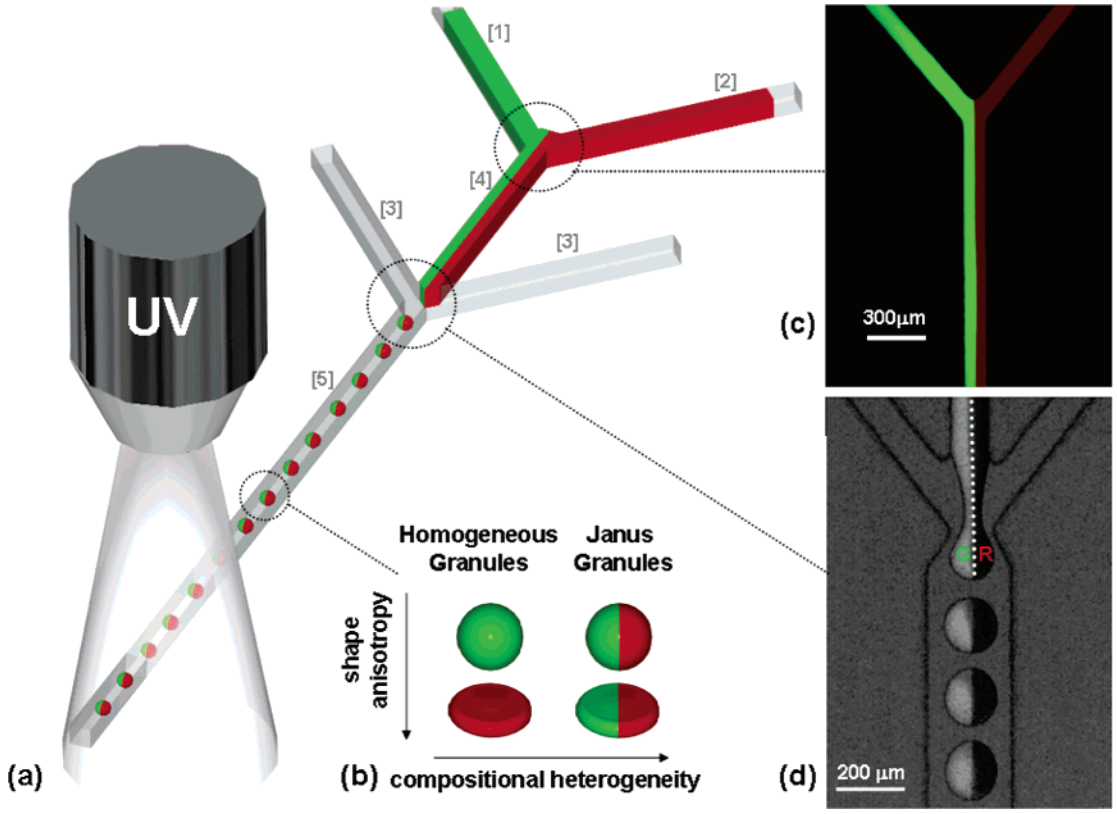

Figure 1. (a) Schematic representation of a sheath-flow microfluidic device used to produce monodisperse colloid-filled hydrogel granules, (b) schematic view of granule shapes and compositions explored, (c) fluorescent image of Y-junction formed by inlets [1] and [2] for the production of Janus spheres, and (d) backlit fluorescence image (green excitation) illustrating that the FITC−silica microspheres remain sequestered in the left hemisphere of each granule generated.

Table 1. Experimental Conditions for Colloid-Filled Hydrogel Granule Production via Microfluidic Assembly

	inlet composition			channel width × height (μm)	
granule composition/shape	[1]	[2]	[3]	[1,2,3,4]	[5]
homogeneous/spherical granules	FITC	FITC	OIL	100 × 150	220 × 150
homogeneous/discoidal granules	RITC	RITC	OIL	100 × 75	220 × 75
Janus/spherical granules	FITC	RITC	OIL	100 × 150	220 × 150
Janus/discoidal granules	FITC	RITC	OIL	100 × 75	220 × 75

of silica microspheres suspended in an aqueous acrylamide solution within a continuous oil phase. The interfacial tension between these two immiscible fluids drives a Rayleigh-mode instability[12,29] that promotes drop formation. Next, the drops undergo photopolymerization to create an acrylamide hydrogel that freezes in the desired morphology and composition during assembly. To demonstrate the flexibility of this new granulation technique, we assemble both spherical and discoid granules of controlled composition.

Experimental Methods

Colloidal suspensions are prepared by adding an appropriate amount of monodisperse silica microspheres ($\phi_{silica} = 0.01-0.45$, 500 ± 25 nm diameter, FUSO, Japan) to an aqueous solution composed of acrylamide ($\phi_{acrylamide} = 0.01-0.3$, Acros Organics), the cross-linker *N*,*N*-methylenebisacrylamide ($\phi_{cross-linker} = 0.001-0.03$, Aldrich), and the photoinitiator 2,2-diethoxyacetophenone (DEAP; $\phi_{initiator} = 0.005$, Aldrich) in deionized water at pH 7 following a procedure similar to that reported in ref 30. To aid direct visualization, silica microspheres (~500 nm in diameter) are synthesized either with a fluorescent, rhodamine isothiocyanate (RITC) or fluorescein isothiocyanate (FITC), core−shell architecture following the procedure described in ref 31. Table 1 contains the inlet compositions used in these experiments, where FITC denotes a 1:1 mixture of pure silica/FITC core−shell silica microspheres, RITC denotes a 1:1 mixture of pure silica/RITC core−shell silica microspheres, and oil refers to a 1:1 mixture of mineral oil (heavy viscosity, PTI Process Chemicals) and hexadecane (H0255, Aldrich) that contains a surfactant (2 wt %, Span 80, Aldrich) and the photoinitiator ($\phi_{initiator} = 0-0.05$). The interfacial tension between the suspension and the oil phase is determined using the pendant drop method[32] and is found to be 10, 4, 3, and 1 mN/m for ϕ_{silica} of 0, 0.15, 0.36, and 0.45, respectively, at a fixed $\phi_{acrylamide}$ of 0.165.

Microfluidic devices are produced via soft lithography[33] by pouring poly(dimethylsiloxane) (Sylgard 184, Dow Corning) onto a silicon wafer patterned with SU-8 photoresist features (Microchem, SU-8 50 for disk-forming channels and SU-8 100 for sphere-forming channels). The microchannel dimensions used in these experiments are provided in Table 1. Monodisperse drops are formed in the sheath-flow microfluidic device illustrated schematically in Figure 1a. The colloidal suspension(s) and oil are loaded into 500 μL glass syringes (1750TTL, Hamilton) and infused into the device via digitally controlled syringe pumps (KDS 100, KD Scientific). The viscosities of a representative colloidal suspension ($\phi_{silica} = 0.36$,

(29) Taylor, G. I. *Proc. R. Soc. London, Ser. A* **1934**, *146* (858), 501−523.
(30) Pan, G. S.; Kesavamoorthy, R.; Asher, S. A. *Phys. Rev. Lett.* **1997**, *78* (20), 3860−3863.
(31) Verhaegh, N. A. M.; van Blaaderen, A. *Langmuir* **1994**, *10*, 1427−1438.
(32) Hansen, F. K.; Rodsrud, G. *J. Colloid Interface Sci.* **1991**, *141* (1), 1−9.
(33) Zhao, X.-M.; Xia, Y.; Whitesides, G. M. *J. Mater. Chem.* **1997**, *7*, 1069−1074.

$\phi_{acrylamide} = 0.165$) and the oil are 9 and 15 cP, respectively, as measured at a strain rate of 250 s^{-1} using a controlled stress rheometer (C-VOR 200, Bohlin). Immediately after each drop is generated, the acrylamide solution is gelled by activating the photoinitiator using a UV lamp with an 8000 mW/cm^2 illumination intensity (N2100 UV lamp, Exfo) that is directed through a 2.5 cm diameter collimating lens (Exfo) at a height of 2 cm above the device surface. We measure the drop gelation time, defined as the UV exposure time required to suppress the Brownian motion of the colloidal particles within them, as a function of acrylamide and initiator concentration. To quantify the extent of polymerization as a function of exposure time, we perform thermogravimetric analysis (TGA) (Pyris 6, Perkin-Elmer) on representative dried granules heated to 800 °C at 10 °C/min in air.

Drop generation is observed using a high-speed camera (Phantom V7.1, Visible Solutions) mounted on an inverted fluorescence microscope (IX-71, Olympus). Direct visualization of both homogeneous and Janus granules is achieved via excitation of the FITC or RITC core−shell silica microspheres using a 100 W Mercury lamp (Chiu Tech. Corp.), whose light was directed through a 500−700 nm (TRITC, Chroma Tech. Corp.) or 450−650 nm (FITC, Chroma Tech. Corp.) filter for red or green excitations, respectively. Representative granules are dried and imaged using scanning electron microscopy (SEM) (6060 LV, JEOL). Image analysis is performed using Image J software on representative wet and dry granule populations (>100 granules) to determine their size distribution. In addition, selected dried granules are freeze-fractured in liquid nitrogen and then imaged using SEM to probe their internal structure.

Results and Discussion

Colloid-filled hydrogel granules are assembled in a sheath-flow microfluidic device with specified shapes and chemical compositions, shown schematically in Figure 1a,b, using the inlet compositions and channel geometries described in Table 1. A fluorescent image of the Y-junction formed at the intersection of inlets [1] and [2] is shown in Figure 1c for the device used to produce Janus granules. The green inlet [1] contains FITC core−shell silica microspheres in suspension, while the red inlet [2] contains RITC core−shell silica microspheres in suspension. A core−shell architecture is adopted for the fluorescent microspheres to eliminate the deleterious interaction between one of the hydrogel constituents and the embedded dye. In these devices, laminar flow and diffusive mixing dominate because of their small channel dimensions and low flow rates. Hence, negligible mixing occurs between the coflowing red and green fluid streams, as evident in Figure 1c.

Further downstream in the device, drops are generated at the modified T-junction formed by the two oil inlets, denoted as [3] in Figure 1a. The width of the necked region where drop formation occurs is adjusted to yield granules approximately 100 μm in diameter (see Figure 1d). Drop formation is driven by the competition between the viscous stress and surface tension between these two immiscible fluids and occurs at a critical capillary number, $Ca = \nu_m \dot{\gamma} R/\sigma$, where $\dot{\gamma}$ is the shear rate at the interface, R is the drop radius, υ_m is the viscosity of the continuous phase, and σ is the interfacial tension between the drop and the continuous phase.[34] Under appropriate conditions, the inner fluid is sheared via external pressure from the continuous phase to an extension long enough to allow surface tension to drive the jet into a drop conformation.[12] As demonstrated previously,[12−14] slight variations in the oil flow rates and channel geometries result in large variations in drop size. For example, when the flow rate of the continuous phase increases, smaller drops form as a result of a greater extension per volume of the inner fluid element.

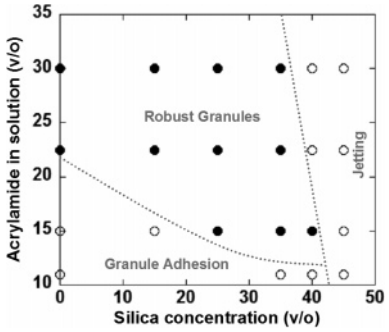

Figure 2. Processing phase diagram outlining the optimal region (filled symbols) for forming robust, monodisperse, colloid-filled hydrogel granules from suspensions of varying composition with fixed photoinitiator concentration ($\phi_{initiator}$ of 0.005 in suspension and $\phi_{initiator}$ of 0.05 in oil) at short UV exposure times (~3 s at an illumination intensity of 8000 mW/cm^2).

To determine the optimal conditions for forming robust colloid-filled hydrogel granules, we investigate the influence of suspension composition on the production of monodisperse granules at fixed flow rates ($Q_{suspension} = 100$ μL/h and $Q_{oil} = 300$ L/h). The results are summarized in the processing phase diagram shown in Figure 2. When the silica volume fraction is relatively high, the suspension breaks in a jetting mode, yielding polydisperse drops as a result of their decreased interfacial tension. When the initial acrylamide concentration is low, significant granule deformation and adhesion occurs upon drying. Thus, an optimal suspension composition of 36 v/o silica and 16.5 v/o acrylamide is identified for the short residence times (~3 s of UV exposure) employed in this device. At this composition, a Ca of 0.07 is required to form granules (~100 μm in diameter) in a dripping mode. Under these conditions, granules are generated at a rate of 45−65 Hz and travel at a velocity of ~6 mm/s.

To prevent the chemically distinct hemispheres of our Janus granules from mixing upon drop breakup, we use a sheath-flow device (Figure 1d) that directs oil flow around the spheres uniformly at breakup. Although the fluid motion within these drops exhibits a recirculatory flow pattern,[16,35] this does not lead to mixing of the hemispheres. However, upon exiting the microchannels, the shear environment changes, thereby promoting mixing of the hemispheres. To immobilize the colloids within each drop, we photopolymerize the aqueous acrylamide solution to form a hydrogel (see Figure 1a). This solidification process preserves both the nonspherical and chemically heterogeneous configurations of the granules, even as they exit the microfluidic device.

To optimize the kinetics of hydrogel formation, we explore the effects of photoinitiator and acrylamide concentration on the polymerization process. Solidification must occur within a few seconds to suppress unwanted mixing or shape changes during assembly given the current device design and flow rates. In preliminary experiments, drops of fixed composition exhibit highly irregular gelation behavior. Such inconsistencies arise because of the solubility of the photoinitiator in the oil phase. The photoinitiator rapidly diffuses from the droplets prior to UV exposure as a result of the enhanced convective diffusion from the fluid recirculation environment.[35] We therefore measure the gelation time, defined as the exposure time at which the Brownian motion of the colloids first ceases, as a function of initiator concentration at a fixed acrylamide concentration. Upon adding a critical concentration of photoinitiator ($\phi_{initiator} \sim 0.05$) to the oil phase, drops are reproducibly and rapidly gelled (<3 s), as

(34) Pathak, J. A.; Migler, K. B. *Langmuir* **2003**, *19*, 8667−8674.

(35) Stone, Z. B.; Stone, H. A. *Phys. Fluids* **2005**, *17*, 063103-1−063103-11.

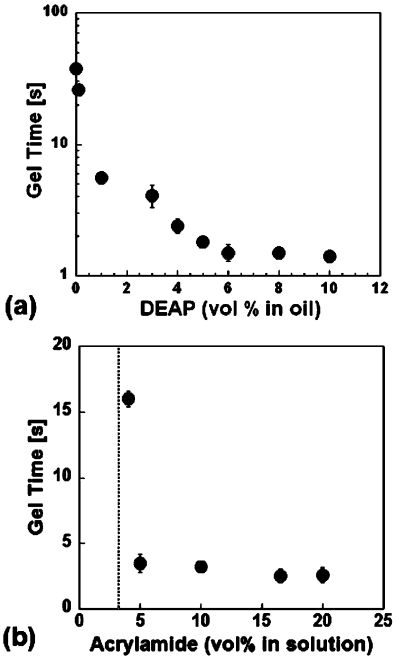

Figure 3. Granule gelation time as a function of (a) DEAP photoinitiator concentration in the oil phase at a fixed $\phi_{acrylamide}$ of 0.165, and (b) acrylamide concentration at a fixed photoinitiator concentration ($\phi_{initiator}$ of 0.005 in suspension and $\phi_{initiator}$ of 0.05 in oil). Gelation is not observed for acrylamide concentrations below ~3 v/o, as indicated by the dashed line in panel b.

shown in Figure 3a. The addition of photoinitiator within the oil phase is essential for maintaining its desired concentration in each drop. Although the use of a more water-soluble photoinitiator would alleviate this need, acetophenone-based species allow more rapid gelation kinetics. We also measure the gelation time as a function of acrylamide concentration at the optimal initiator concentrations of $\phi_{initiator} = 0.005$ in suspension and $\phi_{initiator} = 0.05$ in oil. For initial acrylamide concentrations below approximately $\phi_{acrylamide} = 0.03$, gelation does not occur. At higher initial concentrations, the gelation times decrease from ~20 s for a $\phi_{acrylamide}$ of 0.04 to less than 3 s for a $\phi_{acrylamide}$ of 0.165. For the optimal initial acrylamide concentration, $\phi_{acrylamide} \sim 0.165$, TGA experiments reveal that only 15% of the initial acrylamide in solution polymerizes under these exposure conditions. The excess species are likely removed during the solvent exchange and drying process. To fully polymerize the initial acrylamide in solution, longer exposure times (>10 s) are required.

To demonstrate the flexibility of this new granulation route, we assemble colloid-filled hydrogel granules of varying composition and shape. Specifically, we produce homogeneous and Janus granules in both spherical and discoidal shapes. They are imaged using fluorescence microscopy in the wet state without removal of excess oil (see Figure 4). The characteristic size of the spherical granules is ~110 μm, with a standard deviation of 4.2%. For the discoidal granules, the major and minor axes are ~115 and ~58 μm respectively, resulting in a minor-to-major axis ratio, α, of ~0.50. A coefficient of variation is not reported for these granules because of an insufficient population of discoids that are tilted at appropriate angles for image analysis.

To demonstrate the efficacy of this process as a route for forming robust granules, we harvest and dry the colloid-filled hydrogel granules. It is necessary to exchange the low volatility oil phase with a higher volatility solvent, in this case octane, during the drying process. Pure hydrogel drops (Figure 5a) contract to nearly half of their initial volume upon drying, whereas colloid-filled drops only contract until a random close-packed particle network is formed ($\phi \sim 0.64$).[36] After solvent exchange, we obtain colloid-filled hydrogel granules with relatively smooth

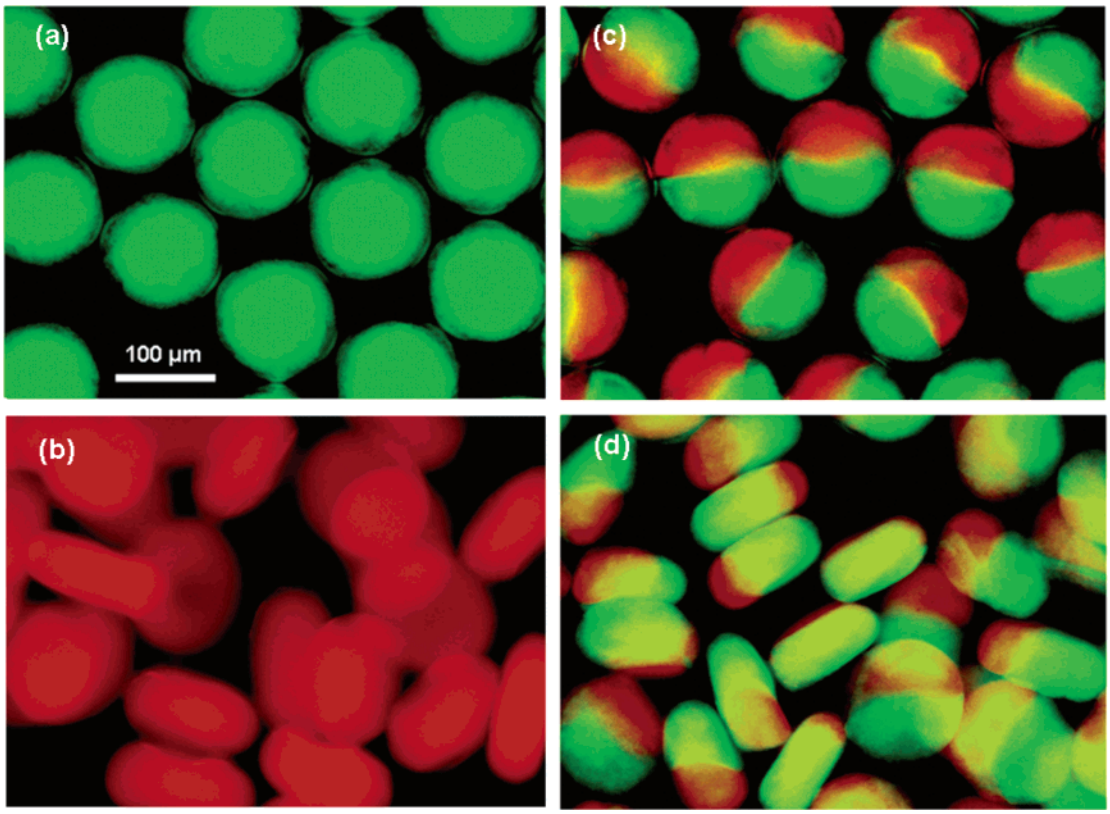

Figure 4. Fluorescence images of homogeneous (a) spherical and (b) discoidal granules (in oil), and two-excitation fluorescence microscopy images of Janus (c) spherical and (d) discoidal granules (in oil). The images acquired from FITC and RITC excitations are overlaid in panels c and d. Scale bars are identical for each image.

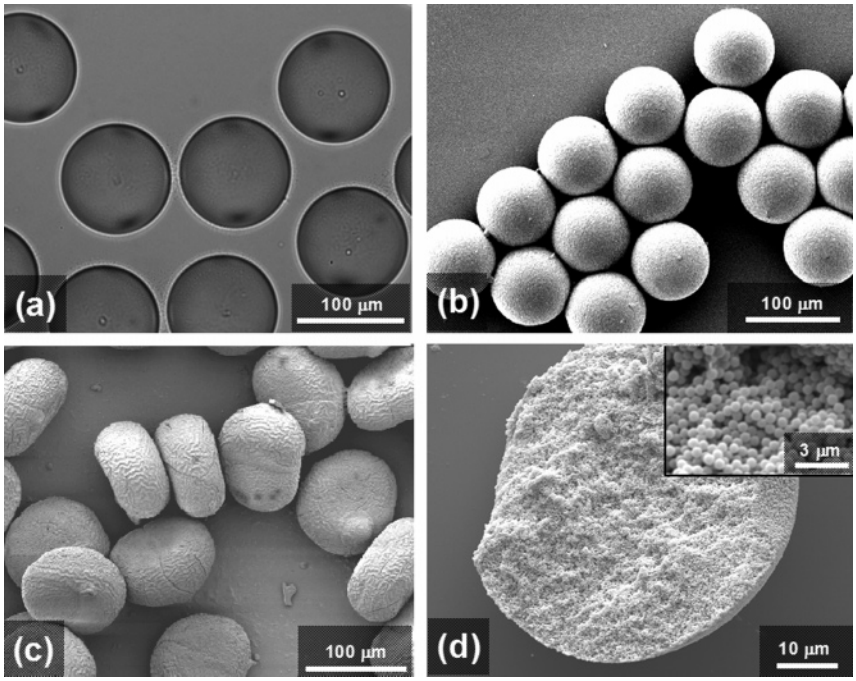

Figure 5. (a) Optical micrograph of pure hydrogel spheres (in oil), (b,c) scanning electron micrographs of dried spherical and discoid granules, and (d) scanning electron micrograph of a dried, freeze-fractured spherical granule. Inset of panel d depicts a higher-magnification view of the random close-packed network of silica microspheres within the dried granule.

surface morphologies. The dried granules retain their spherical (80 μm in diameter) or discoid ($D_{major} = 90\ \mu$m, $D_{minor} = 56\ \mu$m) geometries, as shown in Figure 5b,c. Interestingly, the aspect ratio of the dried discoid granules is slightly higher than that observed in the wet state, although the reason for this anisotropic shrinkage is unclear. Finally, within each dried granule, the silica microspheres assemble into a random close-packed network, as shown in Figure 5d.

Conclusions

Microfluidic-based assembly offers a facile route for assembling monodisperse colloid-filled hydrogel granules of well-controlled size, morphology, and composition. To preserve their structure, we utilize in situ photopolymerization of an acrylamide-based solution during drop generation. For the first time, the production of both homogeneous and hemispherically distinct (Janus) colloidal granules in either spherical or discoidal geometries is demonstrated in the size range relevant for many applications. The ability to tailor the local composition and/or shape of these granular precursors may lead to enhanced packing efficiency[37] and novel applications ranging from ceramics fabrication to pharmaceutical materials.

Acknowledgment. This material is based on work supported by the NSF Center for Nanoscale Manufacturing (Grant # CTS-0120978) and by INEST. The authors thank M. Toepke, K. Ahn, and N. DeForest for useful discussions.

Supporting Information Available: High-speed, backlit fluorescence video of colloid-filled hydrogel (Janus) drop formation as well as time-lapse video microscopy of dried hydrogel drops swelling in the presence of added water. This material is available free of charge via the Internet at http://pubs.acs.org.

LA060759+

(36) Torquato, S.; Truskett, T. M.; Debenedetti, P. G. *Phys. Rev. Lett.* **2000**, *84* (10), 2064−2067.

(37) Donev, A.; Cisse, I.; Sachs, D.; Variano, E. A.; Stillinger, F. H.; Connelly, R.; Torquato, S.; Chaikin, P. M. *Science* **2004**, *303* (13), 990−993.